This is the Pre-Published Version.

S. Zhou, X. Qi, J. Gao, X. Huang, D. Zhang (2023) *Countercurrent Flame Propagation and Quenching Behaviour in a Packed Bed of Spherical PMMA Beads in an Upward Flow of Pure Oxygen*, **Combustion Science and Technology**.
https://doi.org/10.1080/00102202.2022.2160633

Countercurrent Flame Propagation and Quenching Behaviour in a Packed Bed of Spherical PMMA Beads in an Upward Flow of Pure Oxygen

Shuoshuo Zhou[a,b], Xiaobin Qi[a], Jian Gao[a,*], Xinyan Huang[c], Dongke Zhang[a,d]

[a]*Key Laboratory of Biofuels, Qingdao Institute of Bioenergy and Bioprocess Technology, Chinese Academy of Sciences, Qingdao, 266101, China*

[b]*University of Chinese Academy of Sciences, Beijing, 100049, China*

[c]*Department of Building Environment and Energy Engineering, The Hong Kong Polytechnic University, Hong Kong, 999077, China*

[d]*Centre for Energy (M473), The University of Western Australia, 35 Stirling Highway, Crawley, WA 6009, Australia*

[*]Corresponding author: gaojian@qibebt.ac.cn (J Gao)

Abstract

Countercurrent flame propagation and quenching behaviour in a packed bed of spherical polymethyl methacrylate (PMMA) beads in an upward flow of pure oxygen was experimentally studied. Monosized PMMA beads of 2, 5, 8 or 10 mm in diameter (d) were packed in a vertical quartz tube of 35 mm ID to form a bed of 180 mm in height. In a typical experimental run, upon ignition from the top, a blue flame formed and propagated downwards. For d = 10, 8, or 5 mm, there existed a minimum oxygen flow rate (q) to sustain a quasi-steady state flame propagation, and the minimum q increased as d decreased from 10 to 5 mm. However, for d = 2 mm, it was not possible for the flame to propagate downwards irrespective of the q value. The apparent pyrolysis rate (m_{py}) of PMMA was estimated by monitoring the bed mass loss rate, from which the nominal equivalence ratio upon flame quenching was also estimated. The equivalence ratio was found to be less than unity upon flame quenching, suggesting insufficient pyrolysis gases to sustain the combustion. The heat transfer between flame and PMMA bead was analysed theoretically, and it was revealed that the minimum m_{py} to sustain the quasi-steady state flame propagation inversely correlates with the PMMA particle size, and therefore a higher oxygen flow rate is required to sustain the flame propagation in a packed bed of smaller PMMA particles.

Keywords: countercurrent flame propagation; flame quenching; packed bed; PMMA; pyrolysis

1. Introduction

Flame propagation in a packed bed of combustible solid particles is a well-known phenomenon resembling processes encountered in situations such as spontaneous combustion in piles of coal, biomass, and waste (Fatehi and Kaviany, 1994). If the oxidant flow is introduced into the packed bed from the bottom and ignition initiated on the top, the combustion front can propagate downwards against the direction of the oxidant flow, thus termed the countercurrent flame propagation (Fernandez-Pello and Hirano, 1983; Huang and Gao, 2021; Williams, 1977).

A great deal of literature has been devoted to studying the characteristics of and mechanisms driving the countercurrent flame propagation phenomena in a packed bed of particles (Ryu et al., 2006; Yang et al., 2005a; Yang et al., 2005b). Saastamoinen et al. (2000) experimentally found that the countercurrent flame propagation velocity (S_f) increased first and then decreased with increasing airflow rate in a packed bed of wood particles. Shin and Choi (2000) numerically simulated the countercurrent flame propagation process. It was suggested that, as the flow velocity increased, three different modes were experienced in sequence: 1) the oxygen-limited mode, 2) the reaction-limited mode, and 3) the convective cooling mode. S_f would reach a maximum value at the end of the reaction-limited mode, and then decrease in the convective cooling mode due to the enhanced cooling effect of oxidant flow. Such a three-mode rule was further validated by Yang et al. (2004) and Porteiro et al. (2010) in their experiments employed municipal solid wastes and biomass as the solid fuels.

Homogeneous oxidation of the released volatiles and heterogeneous surface oxidation of the char may both contribute to the heat release that sustains the combustion front propagation. As Thunman and Leckner (2002, 2003) suggested, oxygen is preferentially consumed by the volatiles, and therefore heterogeneous surface oxidation of char would be restrained. Our recent work (Qi et al., 2021) indicated that, the competition between the homogeneous and the heterogeneous oxidation would be influenced by the reactivity of the volatiles, and the oxidative reactivity of the volatiles plays an important role. Under the oxygen-limited conditions with a relatively low oxidant flow rate, flaming combustion may transit to glowing combustion (Gao et al., 2021) and further to smouldering combustion (He and Behrendt, 2011; Kadowaki et al., 2021; Yamazaki et al., 2021) for fuels that incur pyrolysis and carbonization such as coal and biomass, which is sustained by the mild heterogeneous surface oxidation of the residue char. However, for plastics such as PMMA, a transition to smouldering is not possible because plastics do not easily carbonize but pyrolyse into gaseous monomers. There should exist a minimum oxidant flow rate to sustain the flame, below which flame quenching occurs. An investigation into the flame quenching is of practical significance, however, systematic studies of quenching of the countercurrent propagating flame in a packed bed are scarce.

Against the above backdrop, the countercurrent flame propagation in a packed bed of monosized spherical beads of PMMA was experimentally examined under the oxygen-limited conditions with relatively low flow rates of pure oxygen in the present work. Particular attention was

given to the flame quenching phenomena. The minimum oxygen flow rate to sustain stable flame propagation was measured for PMMA beads of different diameters. The rate of PMMA pyrolysis was estimated by monitoring the mass loss rate of the packed bed. PMMA is known to easily pyrolyse into gaseous monomers on heating, thus the monitored mass loss should be attributed to PMMA pyrolysis as opposed to its heterogeneous surface oxidation (Zeng et al., 2002). The flame – bead heat transfer was theoretically analysed to aid the interpretation of the experimental results.

2. Experimental

Figure 1 shows a schematic of the experimental setup and a photo of a typical packed bed of spherical PMMA beads. Monosized PMMA beads (d = 2, 5, 8 or 10 mm, respectively) were packed in the vertical quartz tube (I.D. of 35 mm and O.D. of 40 mm) to form a bed of 180 mm in height. The lower part of the tube was filled with ceramic beads (diameter of 2.0 mm) to ensure a uniform gas flow. Pure O_2 metered using a mass flow controller (Seven Star D07-19B), flew through the packed bed from the bottom. Ignition was initiated by placing a burning PMMA bead on the top of the bed. After ignition, a blue flame formed and propagated downwards against to the oxygen flow. When the flame reached the bed of ceramic beads, the experiment was terminated by closing off the oxygen flow.

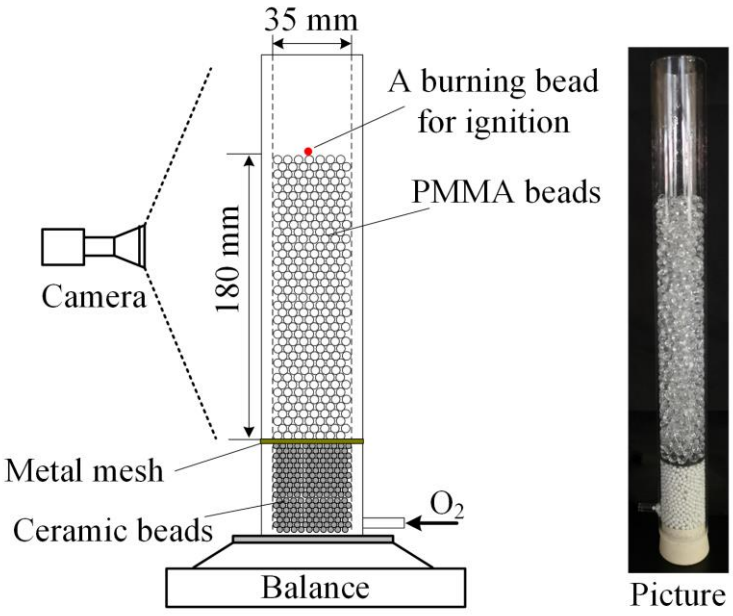

Figure 1 A schematic of the experimental setup

During an experiment, the entire flame propagation process was recorded using a video camera (Sony HDR-CX680) at a rate of 24 frames per second (fps). The images were greyed using the Matlab software and the greyscale of every pixel was obtained. As shown in Fig. 2, for each axial location, the greyscales were averaged along the radial direction, and then the axial location of the maximum average greyscale was deemed as the flame location. The flame propagation velocity was then calculated according to the time sequential flame locations. In the meantime, the instantaneous mass of the entire

packed bed assembly was monitored using an electronic balance with an accuracy of 0.001 g to allow the mass loss rate to be calculated, which is also considered to be the pyrolysis rate m_{py}. The voidage of the water-insoluble PMMA beads packed bed was measured using the water-flooding volume-displacement method. The measured voidage values are 0.402 (± 0.003), 0.427 (± 0.002), 0.452 (± 0.002) and 0.471 (± 0.002), for the beds packed with PMMA beads of 2, 5, 8 and 10 mm in diameter, respectively.

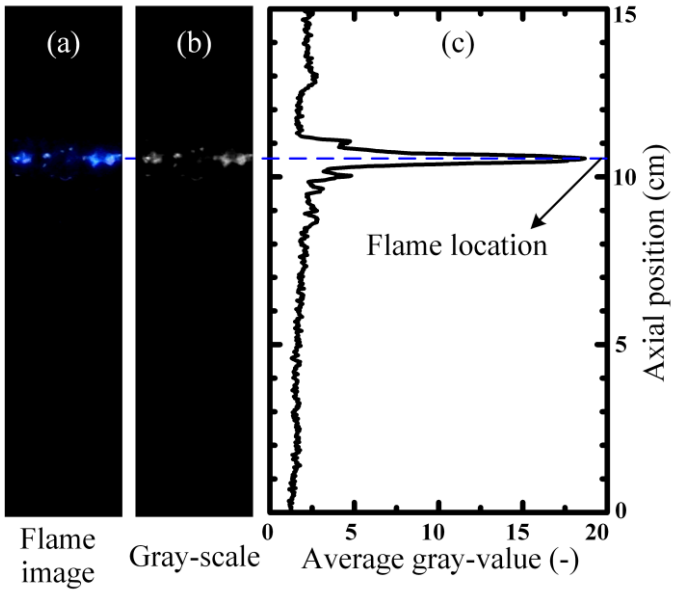

Figure 2 A typical gray-scale image of a propagating flame and the definition of flame location

3. Results and Discussion

3.1 Flame propagation and quenching phenomena

Figure 3(a) shows the time-resolved images recorded for the flame propagation in the packed bed of the PMMA beads with d = 5 mm and at q = 30.1 mL s^{-1}. After ignition, a nearly flat blue flame front forms and propagates downwards. Taking a closer look at the flame front, the bright flame front is actually composed of numerous tiny blue flames. The flame takes about 38 s to propagate to the bottom of the bed, and the measured history of the flame location is shown in Fig. 3(b). The flame location changes with time almost linearly, which can be considered as a quasi-steady state with a constant flame propagation velocity (S_f). S_f estimated according to the slop of the linear fitting curve is about 4.7 mm s^{-1}. Moreover, as shown in Fig. 3(c), the instantaneous bed mass also linearly decreases with time as well. The pyrolysis rate m_{py} is estimated to be 25.6 mg s^{-1}. The total mass consumption of the bed is only 0.94 g, accounting for 0.76% of the initial total bed mass. As a result, the height and structure of the bed remain almost unchanged after the once-through flame propagation process.

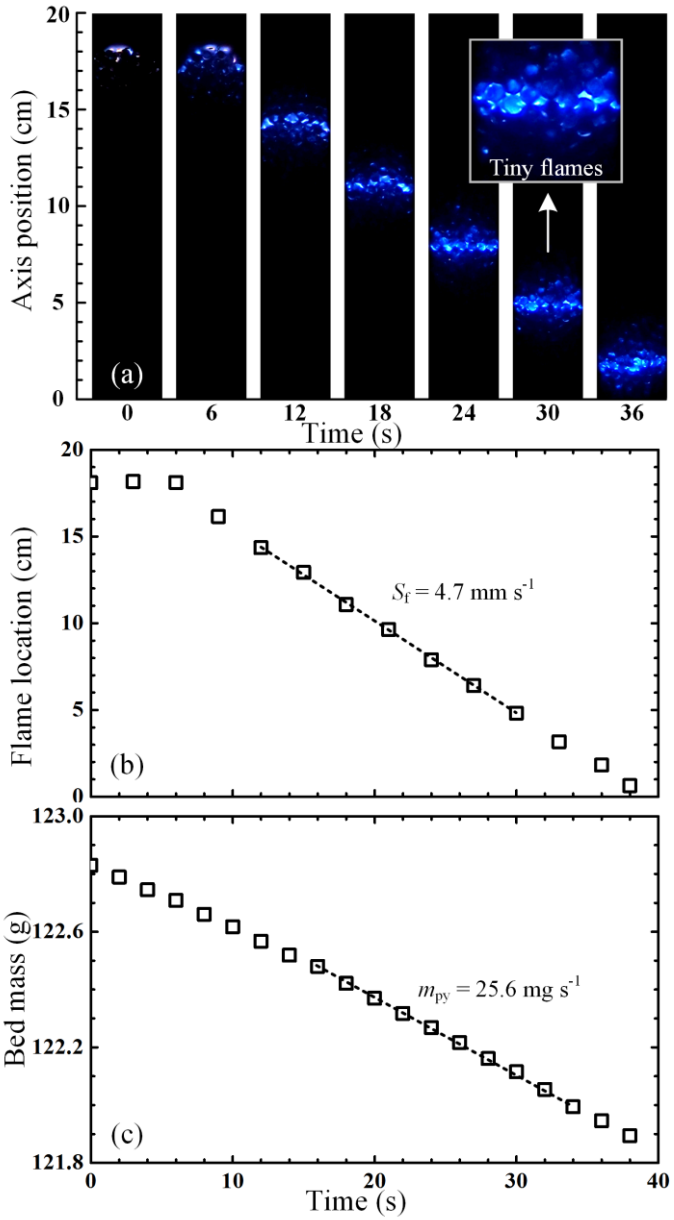

Figure 3 **Typical time-resolved flame images (a), flame location (b), and instantaneous mass of the packed bed (c). PMMA diameter d = 5 mm; Oxygen flow rate q = 30.1 mL s^{-1}**

As q decreases, say, from 30.1 to 22.6 mL s^{-1}, a different "double flame" behaviour was observed. As shown in Fig. 4(a), one flame propagates downwards, leaving the other flame burning at the top of the packed bed. These two flames may be termed as "propagating flame" and "stationary flame", respectively. Comparing Fig. 3(a) and 4(a), it can be seen that the propagating flame becomes weaker as q decreases from 30.1 to 22.6 mL s^{-1}. Figure 4(b) shows that although the propagating flame is still in quasi-steady state, S_f becomes lower than that at q = 30.1 mL s^{-1} (3.0 versus 4.7 mm s^{-1}). Decreasing q weakens the propagating flame, and consequently the upward flowing oxygen is not completely consumed and passes through the downward propagating flame front. The remained oxygen flows upwards and sustains the stationary flame at the bed top. This is the reason why the stationary flame was not observed at $q \geq$ 30.1 mL s^{-1} but appeared at q = 22.6 mL s^{-1}.

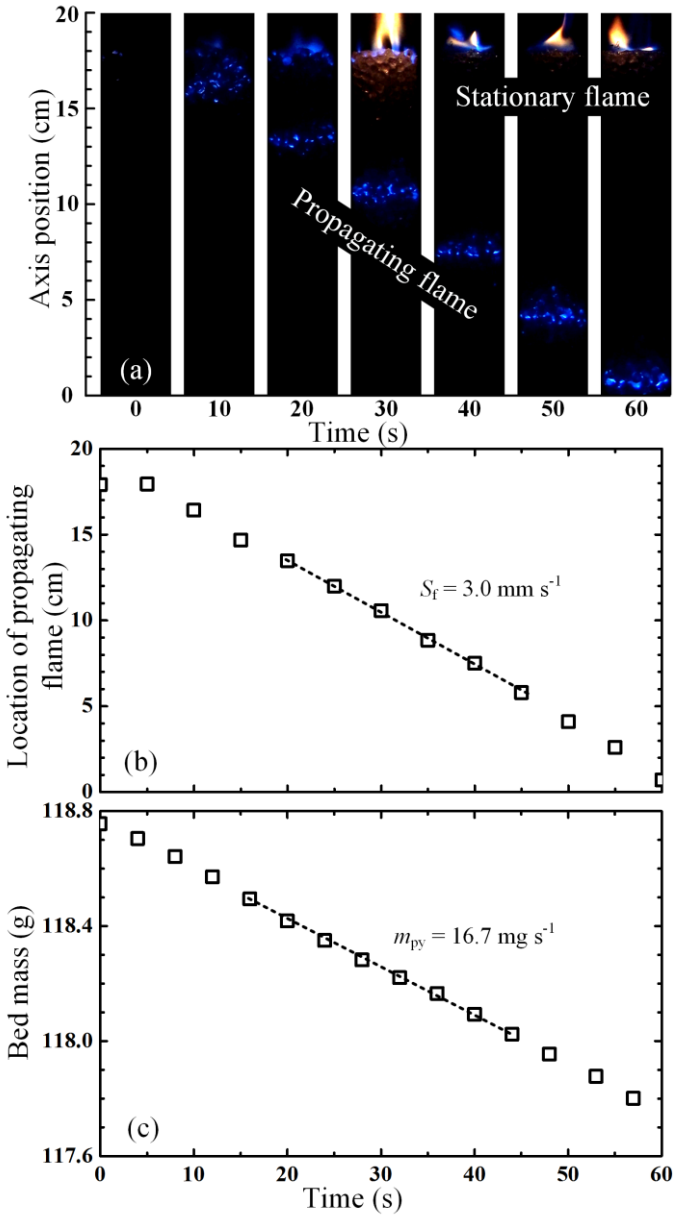

Figure 4 **Typical time-resolved flame images (a), history of flame location (b), and time-resolved profile of bed mass (c). PMMA diameter d = 5 mm; Oxygen flow rate q = 22.6 mL s^{-1}**

Figure 4(c) shows the time-resolved profile of the bed mass. The bed mass loss rate m_{py}, estimated from the slop of the linear fitting curve, was around 16.7 mg s^{-1}. As q further decreases to 18.8 mL s^{-1}, the downward propagating flame was too weak to sustain the propagation and eventually quenched at the axial location of 10 cm after 45 s following ignition, as shown in Fig. 5(a). This means that such a low q cannot sustain the flame propagation in the packed bed with d = 5 mm. Time-resolved flame location and bed mass are shown in Fig. 5(b) and (c), respectively. Figure 6 summarizes the flame propagation velocity at different q with d = 5 mm. As q decreases, S_f decreases, and the minimum q to sustain the quasi-steady state flame propagation was estimated to be 22.6 mL s^{-1}, approximately.

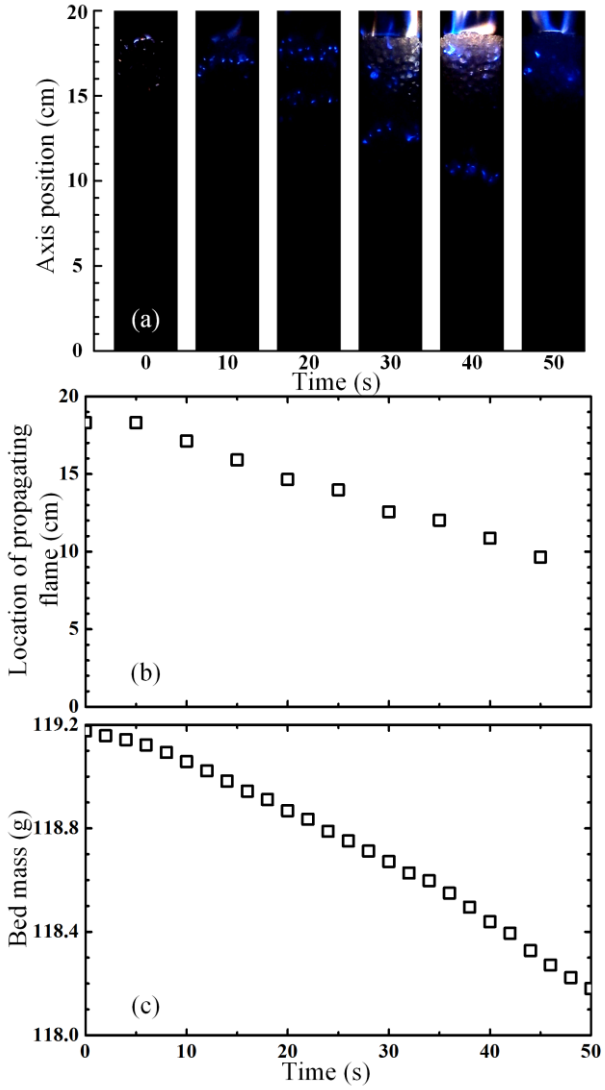

Figure 5 **Typical time-resolved flame images (a), time-resolved flame location (b), and time-resolved profile of bed mass (c). PMMA diameter d = 5 mm; Oxygen flow rate q = 18.8 mL s^{-1}**

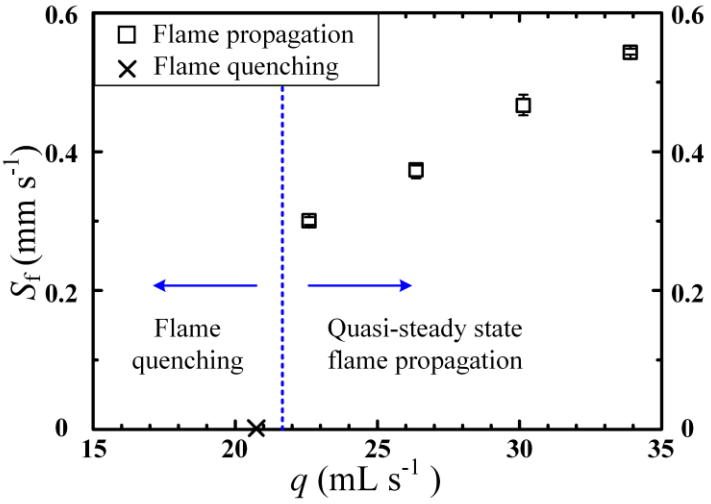

Figure 6 **Flame propagation velocity versus oxygen flow rate in a packed bed of PMMA beads with diameter d = 5 mm**

3.2 Minimum oxygen flow rate and PMMA pyrolysis rate to sustain flame propagation

Flame propagation and quenching characteristics were investigated by performing experiments with d of 10, 8, 5, and 2 mm. A quench event takes place when there is a lack of fuel or oxygen or the temperature is too low. In the present work, the quenching of the countercurrent flame occurred as q decreased leading to a lack of oxygen, or, as d decreased leading to a lack of space or volume to sustain the flame. Figure 7 summarizes the flame propagation and quenching behaviours in the d – q panel. It can be seen that for d = 10 mm, quasi-steady state flame propagation was observed even when q was as low as 1.9 mL s^{-1}. For d = 8 and 5 mm, the minimum q to sustain the quasi-steady state flame propagation are 13.2 and 22.6 mL s^{-1}, respectively. It is therefore indicated that the minimum q increases as d decreases. More interestingly, for d = 2 mm, the flame was not possible to propagate downwards no matter how much q was set to. It implies that, as d decreases to 2 mm, the characteristic bead – bead gap distance may have become too narrow for the flame to pass through, probably due to the severe heat losses from the flame to the PMMA beads. It is suggested that there exists a minimum PMMA bead size, below which self-sustained flame propagation is not possible. Heat loss from the flame to the PMMA beads is believed to be the primary cause of flame quenching, because the PMMA bead surface temperature, which is close to the PMMA pyrolysis temperature of about 630 K (Korobeinichev et al., 2019), is much lower than the flame temperature. In order to further verify the quenching mechanism, additional experiments will be performed in the near future with preheated oxygen flow as the oxidizer.

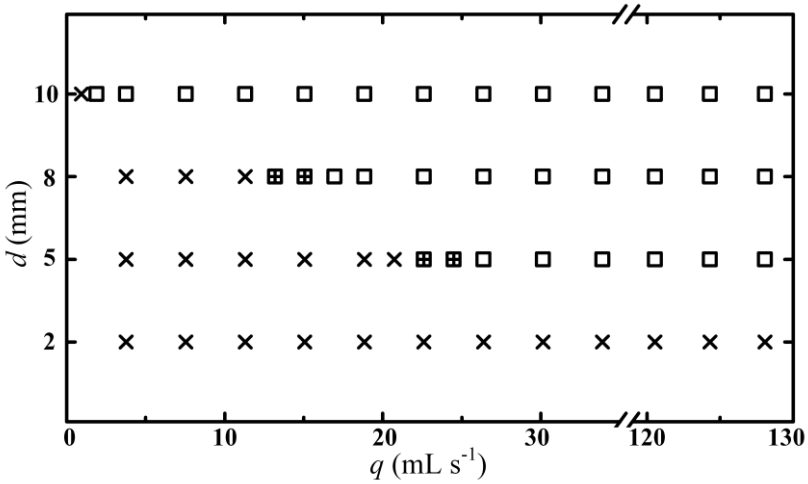

Figure 7 **Flame propagation and quenching behaviours marked in the bead diameter – oxygen flow rate panel. □ - quasi-steady state propagation and no stationary flame; ⊞ - quasi-steady state propagation and stationary flame on the top; × - non-steady state propagation or quenching and stationary flame on the top**

The pyrolysis rate m_{py} can be estimated according to the recorded bed mass history. However, under the conditions with a low q when the propagation flame was about to quench, for example, at q = 22.6 mL s^{-1} with d = 5 mm, the "double flame" mode appeared and therefore the bed mass loss

(pyrolysis) was caused not only by the downward propagating flame by also the stationary flame at the bed top. In order to measure the m_{py} responsible for the downward propagating flame, the stationary flame should be "eliminated". For this purpose, larger beads were stacked at the bed top. For example, as shown in Fig. 8(a), to measure the m_{py} responsible for the downward propagating flame at q = 22.6 mL s^{-1} with d = 5 mm, the larger PMMA beads with d = 8 mm were stacked 40 mm high on the top of the packed bed. Because the top stationary flame would not appear at q = 22.6 mL s^{-1} and d = 8 mm (see Fig. 7), in this way the stationary flame was eliminated. When the flame propagated into the lower part of the bed with d = 5 mm, m_{py} responsible for the downward propagating flame at q = 22.6 mL s^{-1} was successfully measured.

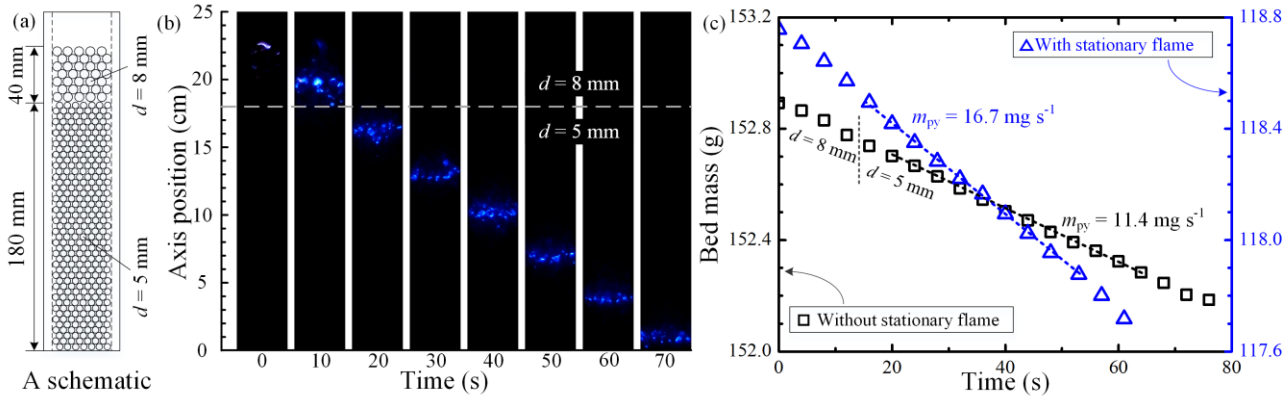

Figure 8 **A schematic (a), time-resolved flame images (b), and time-resolved profile of bed mass (c). For comparison, the time-resolved profile of bed mass with the stationary flame at the bed top is also shown. PMMA diameter d = 5 mm; Oxygen flow rate q = 22.6 mL s^{-1}**

Figure 8(b) and (c) shows the time-resolved flame pictures and the remaining bed mass history, respectively. The m_{py} responsible for the downward propagating flame at q = 22.6 mL s^{-1} and d = 5 mm was about 11.4 mg s^{-1}. For comparison, the time-resolved profile of bed mass with the stationary flame still alight at the bed top is also shown in Fig. 8(c). The estimated pyrolysis rates with and without the stationary flame at the bed top were 16.7 and 11.4 mg s^{-1}, respectively, and therefore the contribution of the stationary flame was estimated to be approximately 5.3 mg s^{-1}, which is a significant contribution to the total pyrolysis rate. Similarly, to measure the m_{py} responsible for the flame propagation in the bed of PMMA beads with d = 8 mm under the near quenching condition at q = 13.2 mL s^{-1}, 40 mm high PMMA beads with d = 10 mm were packed at the bed top to eliminate the top stationary flame. The measured m_{py} for d = 8 and 5 mm are compared in Fig. 9. The minimum m_{py} and q to sustain the quasi-steady state flame propagation with d = 5 mm are 11.4 mg s^{-1} and 22.6 mL s^{-1}, respectively, which are significantly higher than those with d = 8 mm (7.2 mg s^{-1} and 13.2 mL s^{-1}). It is therefore indicated that higher q and m_{py} are required to sustain the flame propagation in a packed bed of smaller fuel particles. To understand the experimental results, flame – bead heat transfer analysis will be performed in the following section.

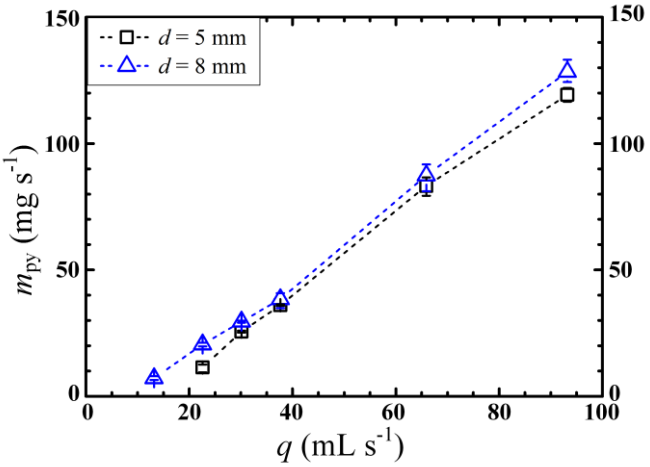

Figure 9 **PMMA pyrolysis rate as a function of oxygen flow rate for the quasi-steady state flame propagation in packed beds of PMMA beads with diameter *d* = 5 and 8 mm, respectively**

3.3 Flame – bead heat transfer analysis

At first, in order to understand the heat transfer process between the flame and the PMMA bead, it is necessary to judge whether the PMMA bead is thermally thick or thin by the Fourier number (*Fo*) and the Biot number (*Bi*). *Fo* and *Bi* for the PMMA bead can be estimated via:

$$Fo = \frac{\lambda_{\mathrm{PMMA}}}{\rho_{\mathrm{PMMA}} c_{\mathrm{p}} S_{\mathrm{f}} d} \tag{1}$$

$$Bi = \frac{hd}{2\lambda_{\mathrm{PMMA}}} \tag{2}$$

where λ_{PMMA} (W m^{-1} K^{-1}), ρ_{PMMA} (kg m^{-3}) and c_{p} (J kg^{-1} K^{-1}) are thermal conductivity, density and specific heat of the PMMA bead, respectively. The convective heat transfer coefficient h (W m^{-2} K^{-1}) can be calculated via (Wakao and Kaguei, 1982):

$$h = Nu \frac{\lambda_{\mathrm{o}}}{\delta} \tag{3}$$

$$Nu = 2 + 1.1 Re^{0.6} Pr^{1/3} \tag{4}$$

where *Nu* is Nusselt number, *Re* is Reynolds number, *Pr* Prandtl number, λ_{o} (W·m^{-1}·K^{-1}) thermal conductivity of the oxygen, δ (m) the characteristic distance of the gap between the PMMA beads. The δ can be estimated by analysing the space structure of the packed bed.

Figure 10(a) illustrates the geometric structure of the packed bed by showing a picture of a number of stuck PMMA beads. The packed bed can be considered as an aggregate of tetrahedron elements and each element consists of four closely packed spherical beads. The flame passed through a gap surrounded by three beads on the same plane, as indicated by the shaded area in Fig. 10(b).

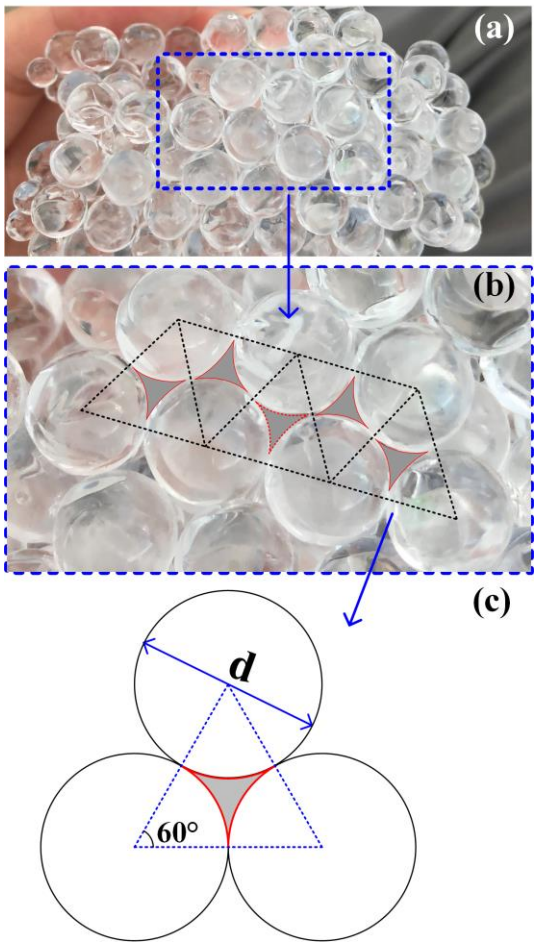

Figure 10 The spatial configuration of a packed bed of PMMA beads

The hydraulic diameter of the shaded area can be considered as the characteristic distance (δ) of the gap for the flame to pass through, which can be calculated as:

$$\delta = 4A_g/C_g \tag{5}$$

where A_g (m^2) and C_g (m) are the area and perimeter of the gap, respectively. Both parameters are related to the diameter of the bead:

$$A_g = \frac{2\sqrt{3}-\pi}{8}d^2 \tag{6}$$

$$C_g = \pi d/2 \tag{7}$$

Combining Eqs. (5-7) yields:

$$\delta = \frac{2\sqrt{3}-\pi}{\pi}d \tag{8}$$

By assuming λ_{PMMA} = 0.19 W m^{-1} K^{-1} (Karpov et al., 2018) and λ_o = 0.074 W m^{-1} K^{-1} at the reference temperature of 1000 K, the estimated *Nu* number, *Fo* number and *Bi* number are *Nu* ≈ 2.8, *Fo* ≈ 0.003, and *Bi* ≈ 5.5, respectively, for the PMMA bead with d = 5 mm at q = 22.6 mL s^{-1}. Such low *Fo*

and high *Bi* indicate that the PMMA bead is thermally thick, and there should exist an apparent temperature gradient within the bead.

According to the pyrolysis rate and oxygen flow rate measured in the experiments, the nominal equivalence ratio (ϕ) can be estimated for judging the flame quenching is caused whether by the lack of fuel or oxygen. Assuming that pyrolysis of PMMA produces a pyrolysis gas with methyl methacrylate (MMA, $C_5H_8O_2$) as the main component. Assuming that oxidation of MMA follows the one-step global reaction:

$$C_5H_8O_2 + 6O_2 = 5CO_2 + 4H_2O \tag{9}$$

The nominal equivalence ratio (ϕ) can be calculated by m_{py} and oxygen mass flow rate m_o.

$$\phi = \frac{(m_{py}/m_o)_{real}}{(m_{py}/m_o)_{stoi}} \tag{10}$$

Figure 11 shows the ϕ as a function of q for the quasi-steady state flame propagation conditions with d = 5 and 8 mm. Interestingly, as q increases, the ϕ first increases and then levels off, approaching characteristic limits of about 1.9 and 2.1 for d = 5 and 8 mm beads, respectively. At a constant oxygen flow rate, the pyrolysis rate as well as the nominal equivalence ratio is comparatively lower for d = 5 mm beads, compared to those for d = 8 mm beads. It is believed that this is because reducing d would cause local flame quenching in the bead-bead gaps, thus restraining pyrolysis at the PMMA bead surface. Under the condition with the minimum q to sustain the quasi-steady state flame propagation, ϕ is 0.75 and 0.80 for d = 5 and 8 mm, respectively. It should be fuel-lean when the flame is nearly quenched, suggesting that the flame quenching is directly caused by the lack of the pyrolysis gas but not oxygen. It is worth noting that for concurrent flame propagation it is fuel-rich with $\phi > 1.0$ under near quenching condition, as recently found by Zhu et al. (2022). The quenching mechanisms for countercurrent and concurrent flame propagation may be different and therefore warrant a further comparative investigation.

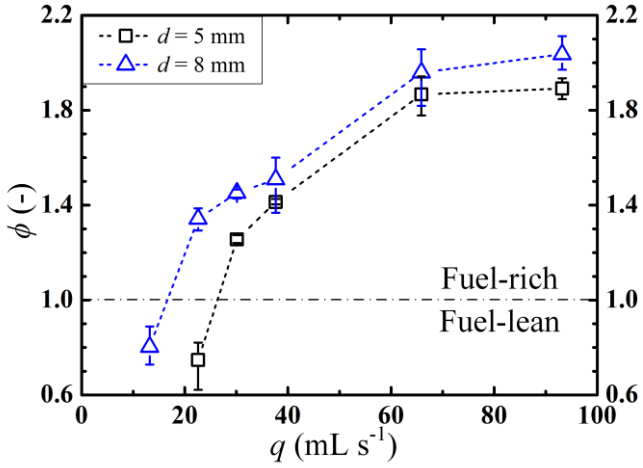

Figure 11 **Estimated nominal equivalence ratios at different oxygen flow rates for the quasi-steady state flame propagation in packed beds of PMMA beads with diameter d = 5 and 8 mm, respectively**

The lack of the pyrolysis gas invokes that the combustion heat release rate (Q_c) can be estimated via:

$$Q_c = m_{py}\Delta H_c \tag{11}$$

where m_{py} (kg s^{-1}) is the fuel pyrolysis rate, and ΔH_c (J kg^{-1}) the combustion heat of MMA. A certain amount of combustion heat contributes to sustaining the pyrolysis of PMMA to release the combustible gas (MMA), and therefore the net heat generation rate (Q_{net}) should be:

$$Q_{net} = m_{py}(\Delta H_c - \Delta H_{py}) \tag{12}$$

where ΔH_{py} (J kg^{-1}) is the pyrolysis heat of PMMA. Under the condition where the flame is about to quench,

$$m_{py} = m_{py,min} \tag{13}$$

where $m_{py,min}$ is the minimum pyrolysis rate to sustain the quasi-steady state flame propagation. According to the experiments, the flame appeared blue and not sooty, so that it is reasonable to assume convection dominates the heat transfer between the flame and the PMMA beads and radiation is negligible (Zhou et al., 2022). The net heat generated preheats the PMMA beads via convection, and therefore:

$$m_{py,min}\left(\Delta H_c - \Delta H_{py}\right) = Q_{conv} \tag{14}$$

The convective heat transfer between the flame and the PMMA bead surface can be estimated via:

$$Q_{conv} = L_f A' h\left(T_f - T_{py}\right) \tag{15}$$

where L_f (m) is the height of the combustion zone, A' (m^2 m^{-1}) surface area per height, h (W m^{-2} K^{-1}) convective heat transfer coefficient, T_f (K) flame temperature, and the temperature at the surface of PMMA bead is assumed to the pyrolysis temperature of PMMA T_{py} (K) (assumed to be a constant at about 630 K according to Korobeinichev et al. (2019)).

Assuming that the beads are arranged in the close-packed structure and ignoring the boundary effect, the surface area per height (A') in the packed bed can be calculated as follows. The surface area of a PMMA bead is: $A_{PMMA} = \pi d^2$. The cross sectional area of the packed bed with inner diameter D is: $A_b = \pi D^2/4$. Figure 9 shows that each PMMA bead is surrounded by six beads on the same plane. Because the area of the circumscribed regular hexagon of of a circle with diameter d is $A_h = \sqrt{3}d^2/2$, the number of PMMA beads on the same horizontal plane is A_b/A_h. Therefore, the total surface area of these beads is:

$$A = A_{PMMA} \cdot A_b/A_h = \frac{\sqrt{3}}{6}\pi^2 D^2 \tag{16}$$

The height occupied by the beads on the same horizontal plane is:

$$H = \sqrt{3}d/2 \tag{17}$$

Combining Eqs. (16-17) yields:

$$A' = \frac{A}{H} = \frac{\pi^2 D^2}{3d} \tag{18}$$

Submitting Eqs. (3, 8, 18) into Eq. 15 yields:

$$Q_{\text{conv}} = \frac{\pi^3 D^2 L_f \lambda_o Nu(T_f - T_{py})}{3(2\sqrt{3}-\pi)d^2} \tag{19}$$

Combining Eqs. (14, 19) yields:

$$m_{py,\min} = \frac{\pi^3 D^2 L_f \lambda_o Nu(T_f - T_{py})}{3(2\sqrt{3}-\pi)d^2(\Delta H_c - \Delta H_{py})} \tag{20}$$

Assuming that T_f is constant and L_f is proportional to the characteristic distance (δ) of the gap between the PMMA beads (thus proportional to d according to Eq. 8), from Eq. 20, it is therefore deduced that

$$m_{py,\min} \propto 1/d \tag{21}$$

showing an inversely proportional correlation between d and m_{py}. The experimental finding that the minimum pyrolysis rate increases as d decreases from 8 to 5 mm is therefore validated. Sustaining flame propagation in packed bed of smaller PMMA particles requires a higher pyrolysis rate fulfilled by a higher oxygen flow rate.

4. Conclusions

Countercurrent flame propagation and quenching phenomena in a packed bed of PMMA beads were experimentally observed and systematically analysed. After ignition on the top of the bed, a blue flame formed and propagated downwards in a quasi-steady state. It was found that the minimum oxygen flow rate to sustain the quasi-steady state flame propagation increased as the PMMA bead diameter (d) decreased from 10 to 5 mm. For d = 2 mm, however, the flame was not able to propagate downwards regardless of the flow rate. The nominal equivalence ratio was calculated based on the set oxygen flow rate and estimated PMMA pyrolysis rate. The nominal equivalence ratio was found to be less than unity under the conditions when the flame was about to quench, suggesting that the flame quenching was probably caused by the lack of fuel gas from PMMA pyrolysis. The flame – bead heat transfer analysis suggested that the minimum PMMA pyrolysis rate to sustain the quasi-steady state flame propagation is inversely proportional to the PMMA bead size, and therefore a higher oxygen flow rate was required to sustain the flame propagation in a packed bed of smaller PMMA particles.

Acknowledgement

This work has received funding support from the National Natural Science Foundation of China (No. 51806230 and 51906251), Australian Research Council (ARC DP210103766 and DP220100116) and the Future Energy Export Cooperative Research Centre (FEnEx CRC Project# 21.RP2.0059). The start-up financial support from QIBEBT, CAS provided to the Thermal Energy Engineering Team is also acknowledged.

References

Fatehi, M., and Kaviany, M. 1994. Adiabatic Reverse Combustion in a Packed Bed. *Combust. Flame*, ***99***, 1.

Fernandez-Pello, A.C., and Hirano, T. 1983. Controlling Mechanisms of Flame Spread. *Combust. Sci. Technol.*, ***32***, 1.

Gao, J., Qi, X., Zhang, D., Matsuoka, T., and Nakamura, Y. 2021. Propagation of Glowing Combustion Front in a Packed Bed of Activated Carbon Particles and the Role of Co Oxidation. *Proc. Combust. Inst.*, ***38***, 5023.

He, F., and Behrendt, F. 2011. Experimental Investigation of Natural Smoldering of Char Granules in a Packed Bed. *Fire Saf. J.*, ***46***, 406.

Huang, X., and Gao, J. 2021. A Review of near-Limit Opposed Fire Spread. *Fire Saf. J.*, ***120***, 103141.

Kadowaki, O., Suzuki, M., Kuwana, K., Nakamura, Y., and Kushida, G. 2021. Limit Conditions of Smoldering Spread in Counterflow Configuration: Extinction and Smoldering-to-Flaming Transition. *Proc. Combust. Inst.*, ***38***, 5005.

Karpov, A.I., Korobeinichev, O.P., Shaklein, A.A., Bolkisev, A.A., Kumar, A., and Shmakov, A.G. 2018. Numerical Study of Horizontal Flame Spread over Pmma Surface in Still Air. *Appl. Therm. Eng.*, ***144***, 937.

Korobeinichev, O.P., Paletsky, A.A., Gonchikzhapov, M.B., Glaznev, R.K., Gerasimov, I.E., Naganovsky, Y.K., Shundrina, I.K., Snegirev, A.Y., and Vinu, R. 2019. Kinetics of Thermal Decomposition of Pmma at Different Heating Rates and in a Wide Temperature Range. *Thermochim. Acta*, ***671***, 17.

Porteiro, J., Patiño, D., Collazo, J., Granada, E., Moran, J., and Miguez, J.L. 2010. Experimental Analysis of the Ignition Front Propagation of Several Biomass Fuels in a Fixed-Bed Combustor. *Fuel*, ***89***, 26.

Qi, X., Zhou, S., Gao, J., Zhu, M., Zhang, Z., and Zhang, D. 2021. Counter-Current Flame Propagation in a Cylindrical Bed of Activated Carbon Saturated with Artificial Volatile Matter in an Upward Flow of O2/N2 Mixture. *Proc. Combust. Inst.*, ***38***, 4251.

Ryu, C., Yang, Y.B., Khor, A., Yates, N.E., Sharifi, V.N., and Swithenbank, J. 2006. Effect of Fuel Properties on Biomass Combustion: Part I. Experiments—Fuel Type, Equivalence Ratio and Particle Size. *Fuel*, ***85***, 1039.

Saastamoinen, J.J., Taipale, R., Horttanainen, M., and Sarkomaa, P. 2000. Propagation of the Ignition Front in Beds of Wood Particles. *Combust. Flame*, ***123***, 214.

Shin, D., and Choi, S. 2000. The Combustion of Simulated Waste Particles in a Fixed Bed. *Combust. Flame*, ***121***, 167.

Thunman, H., and Leckner, B. 2002. Modeling of the Combustion Front in a Countercurrent Fuel Converter. *Proc. Combust. Inst.*, ***29***, 511.

Thunman, H., and Leckner, B. 2003. Co-Current and Counter-Current Fixed Bed Combustion of Biofuel—a Comparison. *Fuel*, ***82***.

Wakao, N., and Kaguei, S. 1982. *Heat and Mass Transfer in Packed Beds*, Gordon and Breach Science Publishers, New York.

Williams, F.A. 1977. Mechanisms of Fire Spread. *Symp. (Int.) Combust.*, ***16***, 1281.

Williams, F.A. 1985. *Combustion Theory*.

Yamazaki, T., Matsuoka, T., Kuwana, K., and Nakamura, Y. 2021. Study on the Flaming-Transition Behavior of a Downwardly Smoldering Biomass Stick Utilizing Low Pressure. *Proc. Combust. Inst.*, ***38***, 5073.

Yang, Y., Ryu, C., Khor, A., Sharifi, V., and Swithenbank, J. 2005a. Fuel Size Effect on Pinewood Combustion in a Packed Bed. *Fuel*, ***84***, 2026.

Yang, Y., Ryu, C., Khor, A., Yates, N., Sharifi, V., and Swithenbank, J. 2005b. Effect of Fuel Properties on Biomass Combustion. Part Ii. Modelling Approach—Identification of the Controlling Factors. *Fuel*, ***84***, 2116.

Yang, Y.B., Sharifi, V.N., and Swithenbank, J. 2004. Effect of Air Flow Rate and Fuel Moisture on the Burning Behaviours of Biomass and Simulated Municipal Solid Wastes in Packed Beds. *Fuel*, ***83***, 1553.

Zeng, W.R., Li, S.F., and Chow, W.K. 2002. Preliminary Studies on Burning Behavior of Polymethylmethacrylate (Pmma). *J. Fire Sci.*, ***20***, 297.

Zhou, S., Gao, J., Wu, J., and Zhang, D. 2022. Countercurrent Flame Propagation inside Vertical Pmma Cylinders against Pure Oxygen Flow. *Combust. Flame*, ***246***, 112396.

Zhu, F., X. Huang, X. Chen, and S. Wang. 2022. *Flame spread transition to regression of thick fuel in oxygen-limited concurrent flow*. Fire Technology. Accepted.